Influence of surface chemistry on the transport of H atoms in a supersonic hydrogen plasma jet

S. Mazouffre,[a] P. Vankan, R. Engeln, and D. C. Schram
Department of Applied Physics, Eindhoven University of Technology, P.O. Box 513, 5600 MB Eindhoven, The Netherlands

(Received 21 February 2001; accepted 23 May 2001)

The transport of ground-state hydrogen atoms in the expansion of a thermal hydrogen plasma created by a cascaded arc is studied by means of two-photon absorption laser induced fluorescence. The low-dissociation degree measured at the source exit implies that H atoms flow in a H_2 environment. It is shown that the H atom expansion pattern is in disagreement with the neutral gas supersonic expansion theory. Indeed the transport of H atoms in the plasma jet is strongly influenced by surface-recombination processes. Because of the large density gradients between the core of the jet and its surroundings induced by the recombination of H atoms at the reactor walls, hydrogen atoms diffuse out of the plasma jet in the course of the expansion. When the surface loss probability is high, i.e., the combination of a large wall-recombination probability with a long residence time, the losses of radicals by diffusion cannot be avoided even when the mass of the carrier gas is close to the mass of the radical. © *2001 American Institute of Physics.* [DOI: 10.1063/1.1385520]

I. INTRODUCTION

The study of hydrogen plasma expansions is, in the first place, of particular interest, since it concerns many different systems that cover a broad range of dimensions. Hydrogen being the most abundant form of matter in the universe, objects like solar flares and phenomena like solar wind and supernovae represent examples of astrophysical-scale, expanding hydrogen plasma.[1] At intermediate scale, hydrogen expansions are found in systems like the divertor region of a tokamak plasma (see, for example, Ref. 2) and the remote plasma jets used for surface modification.

In the second place, hydrogen plasma expansions contain light and highly reactive hydrogen atoms, which play a key role in many chemical reactions encountered in plasma processes. To clearly demonstrate the importance of H atom chemistry, two examples will be given that are associated with energy and environmental problems humanity has to face in the next century. Hydrogen atoms are involved in the plasma-aided fast deposition of thin films of hydrogenated amorphous silicon (a-Si:H) needed for the next solar cell generation.[3] Atomic hydrogen radicals control the growth process and thus the final film properties. In the field of controlled nuclear fusion, atomic hydrogen plays a specific role. First, one wants to use H atom sources for neutral beam heating of fusion devices (mainly via the production of negative hydrogen ions H^{-}[4]). Second, the interaction of H atoms with the reactor surfaces and the resulting reaction products, i.e., H_2 molecules, have drastic consequences on the stability of the plasma, and therefore, on device performances.[5,6] Numerous works are nowadays devoted to this so-called hydrogen recycling process and they all require the development of plasma sources capable of generating a high H atom flux.

All aforementioned processes are to a large extent governed by the transport mechanisms of H atoms in an expanding hydrogen plasma. In view of the applicability, it is therefore of importance to study the H atom flow pattern, as well as the influence of plasma–wall interactions on the transport properties. Moreover, the study of a plasma expansion at a specific scale may serve as an example, and the results obtained can be generalized to any kind of plasma expansion with larger and smaller scales. On a more fundamental point of view, this study serves as a test case to find new evidence to confirm the fact that a radical expansion can differ strongly from a neutral gas expansion. This anomalous transport of radicals in a plasma jet, induced by wall-recombination phenomena, has been reported recently in the case of an $Ar–H_2$ and $He–H_2$ mixture.[7,8] In a hydrogen expansion, the mass of the carrier gas is close to that of the radical, and the resulting enhancement of confinement especially is of interest.

In the experiments reported here, ground-state hydrogen atoms are spatially probed using a two-photon excitation laser-induced fluorescence technique (TALIF) in an expanding thermal hydrogen plasma produced by a cascaded arc. The determination of the atomic hydrogen density, temperature, and velocity profiles enable to investigate in detail the transport mechanisms of H atoms in a supersonic plasma jet. The paper is organized as follows. Section II describes briefly the hydrogen supersonic plasma jet and the experimental arrangement. A summary of the outcomes of coherent anti-Stokes Raman scattering (CARS) measurements performed on an expanding hydrogen plasma is also given in this paragraph. In Sec. III, axial profiles of both H and D density and temperature are presented which reveal losses of H atoms during the expansion process. In Sec. IV, the observed low dissociation degree at the arc outlet is discussed in terms of surface-recombination of H atoms in the arc nozzle. Velocity profiles along the jet axis are given in Sec.

[a]Electronic mail: s.mazouffre@phys.tue.nl

V, and the shock wave structure is explained. In Sec. VI, a measured cross section of the jet reveals as expected a low H density around the plasma jet. Finally, conclusions are given in Sec. VII.

II. EXPERIMENTAL ARRANGEMENT AND CARS MEASUREMENTS

A. Plasma source and plasma jet

The hydrogen plasma is created by a cascaded arc.[9] The arc channel is composed of four insulated plates and has a diameter of 4 mm. The operating standard conditions are: A 55 A direct current (dc), a cathode-anode voltage of 150 V and a H_2 gas flow of 3.5 standard liters per minute (slm). The stagnation pressure inside the arc is 0.14 bar. The thermal hydrogen plasma expands from a straight nozzle with a diameter of 4 mm into a roots-blower pumped vacuum vessel where the background pressure (p_{back}) can be varied, almost independently from the gas flow, from 10 to 10^5 Pa (atmospheric pressure). The cascaded arc plasma source is mounted on a translation arm. Spatial scans through the expanding plasma can be performed by moving the arc relative to the intersection of laser beam and detection volume ($0.1\times1\times1$ mm^3).

Since in this contribution we focus on the transport of H atoms, it is of interest to briefly present the ways H atoms can be produced in the plasma source where the electron temperature T_e is around 1 eV. Ground-state atomic hydrogen can be generated by direct dissociation of H_2 molecule by electron impact

$$e + H_2 \rightarrow H + H + e. \tag{1}$$

Yet the rate coefficient is relatively low at 1 eV.[10–12] Another possibility is the dissociative recombination of molecular ions

$$e + H_2^+ \rightarrow H^* + H \quad \text{and} \quad e + H_3^+ \rightarrow H + H + H. \tag{2}$$

Both reactions are fast at low T_e.[12] Note that H_2^+ can easily form H_3^+ when reacting with H_2 and this again leads to the formation of a H atom

$$H_2^+ + H_2 \rightarrow H_3^+ + H. \tag{3}$$

Another mechanism of interest for the H atom production is the charge transfer between a proton and a rovibrationally excited hydrogen molecule[13,14]

$$H_2^{v,J} + H^+ \rightarrow H_2^+ + H. \tag{4}$$

The excited molecules are necessary to make the reaction exothermic. The energy deficit being around 2 eV, the charge exchange process is strongly favored for $H_2(v \geqslant 4)$. Note that the dissociation by impact with a proton of the H_2 molecule to form two H atoms is also possible at high v number.[13] The foregoing reactions have been proposed to explain the anomalous ion recombination, i.e., the fast ionization loss, in the expansion of a hydrogen plasma created by a cascaded arc.[14] Indeed without any influence of the arc parameters the plasma emerging from a cascaded arc with a straight nozzle is dark, which means that it contains mainly neutral particles, i.e., H atoms and H_2 molecules in our case. As measured by Thomson scattering, the ionization degree at the arc exit is less than 1%.[15]

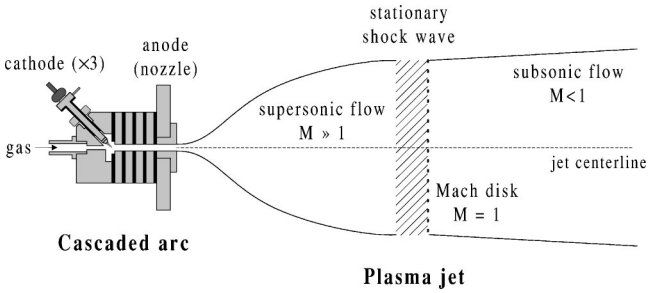

FIG. 1. The cascaded arc and simplified structure of an expanding plasma jet. The plasma first expands supersonically from a straight nozzle. At some distance from the source a shock wave is created to allow the flow to adapt to the local conditions. Behind the shock region the plasma flows subsonically and at constant static pressure.

A detailed description of the dynamics of an expanding gas or plasma can be found elsewhere.[8,16,17] Here only a short overview of the expansion picture is presented. Because the plasma expands through a nozzle from a high-pressure region (source) into a low-pressure region, a well-defined, free-jet shock wave structure is produced, as schematically depicted in Fig. 1. The plasma first expands supersonically. In this flow regime, the drift velocity increases and due to energy conservation the temperature drops in accordance with the Poisson adiabatic law. The particle density along a stream line decreases because of the increase in the jet diameter (rarefaction effect). At some distance from the source, depending on the source stagnation pressure (p_o) and on the background pressure (p_{back}), a stationary shock wave is formed to allow the flow to adapt to the ambient gas conditions.[18] The Mach disk location z_M (position at which the Mach number is equal to 1) is given by[16,17]

$$z_M = 0.7d\sqrt{\frac{p_o}{p_{\text{back}}}}, \tag{5}$$

where d is the nozzle diameter ($d=4$ mm). Throughout the shock region, where dimensions are in the order of the local neutral–neutral collision mean free path, the flow undergoes a transition from a supersonic regime to a subsonic regime. Behind the shock wave, the plasma flows at constant static pressure. As we will see in the next sections, the transport of H atoms in an expanding hydrogen plasma jet is clearly in disagreement with the classical neutral gas expansion theory.

B. Optical system

In the experiment reported in this contribution, ground-state hydrogen atoms are spatially probed by using a two-photon absorption laser-induced fluorescence (TALIF) technique.[19,20] Only a short overview of the experimental method is presented here. A simplified scheme of the setup is depicted in Fig. 2. A tunable 20 Hz Nd:YAG pumped dye laser delivers radiation around 615 nm. The output of the dye laser is frequency-tripled using nonlinear optical crystals resulting in 2 mJ of tunable ultraviolet (UV) light around

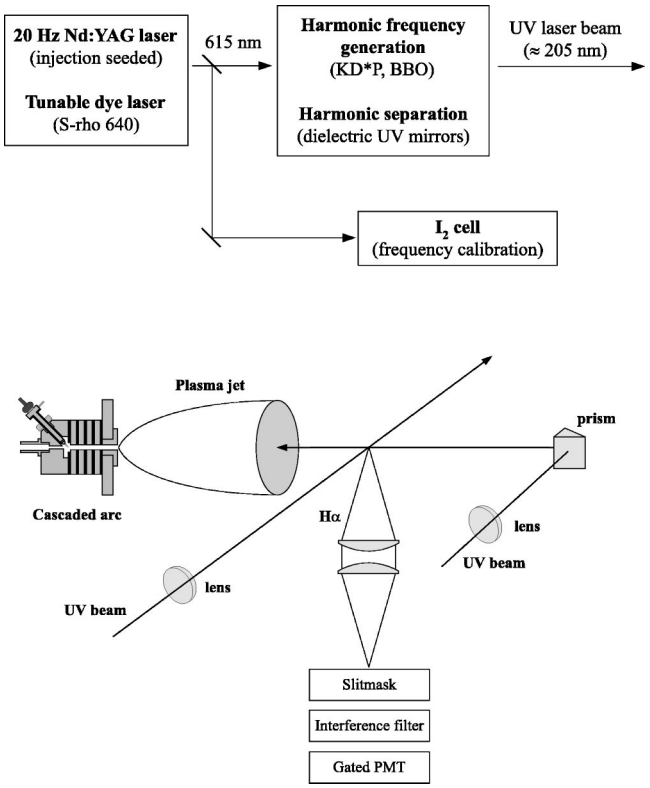

FIG. 2. Schematic view of the experimental arrangement. Top picture: Laser system used to generate pulsed tunable UV radiation around 205 nm. Bottom picture: Configuration of the excitation branch and of the H_α fluorescence detection branch. The UV laser beam can be directed either perpendicular or parallel to the plasma flow which allows for the measurement of $(T_\perp, w_r)$ and $(T_\parallel, w_z)$, respectively.

205 nm with a measured bandwidth of 0.2 cm^{-1}. The UV laser beam is focused into the vacuum chamber either perpendicular or parallel to the plasma expansion axis, see Fig. 2. In the latter case the optics are located in the vacuum chamber and protected from the plasma flow by means of a water cooled screen. Hydrogen atoms are excited with two 205 nm photons from the $1s^2S$ ground state to the $3d^2D$ and $3s^2S$ states. The excitation is monitored by detection of the resulting fluorescence yield on the Balmer-α line at 656 nm using a gated photo-multiplier tube (PMT). A bandwidth interference filter ($\Delta\lambda = 10$ nm) is used to isolate the H_α line from the plasma emission. A slitmask is used to define the detection volume, the dimensions of which are smaller than any gradient length. The PMT signal is recorded by means of an oscilloscope connected to a computer. The dye-laser frequency is calibrated by the simultaneous recording of the absorption spectrum of molecular iodine. From a spectral scan over the two-photon transition, the local H atom density, temperature (perpendicular and parallel to a stream line), and velocity (radial and axial component) are determined.

Absolute number densities are obtained by calibrating the H atom fluorescence yield using a known amount of krypton gas.[21] The krypton atom has a two-photon excitation scheme very similar to that of H. Furthermore, the ratio of the two-photon absorption cross section of Kr to H has been accurately measured.

C. CARS measurements on an expanding hydrogen plasma

The expansion of a thermal hydrogen plasma created by a cascaded arc has already been investigated using the coherent anti-Stokes Raman scattering (CARS) diagnostic.[22] A CARS setup has been built in order to locally measure the rotational and vibrational temperature as well as the absolute density of H_2 molecules in the plasma jet. The arc configuration and the H_2 gas flow are identical to the ones used in that work. The arc current was 40 A. We here shortly summarize the main results of the CARS measurements. This is useful to compare the transport of H atoms with the transport of H_2 molecules in the expansion. Furthermore, as will be discussed in Sec. IV, the combination of the CARS and the TALIF results open the way to explain the low ionization and the low-dissociation degree measured at the arc exit.

The plasma appears to be mainly composed of ground-state H_2 molecules. The measurements clearly reveal the absence of significant amounts of rovibrationally excited hydrogen molecules in the jet. At $z=20$ mm the density of $H_2(v=0)$ is equal to 1.4×10^{21} m^{-3}, the density of $H_2(v=2)$ is approximately 10^{18} m^{-3} and the density of $H_2(v=4)$ is less than 10^{17} m^{-3}. Unfortunately, the CARS measurements could not be performed at the arc exit because of the crossed laser beam geometry and thus information concerning the energy distribution of H_2 molecules leaving the arc is still lacking.

At $z=20$ mm, the total H_2 density n_{H_2} is equal to approximately 2×10^{21} m^{-3} and the rotational temperature T_{rot} is equal to 1400 K. In the subsonic domain, the H_2 static pressure is constant and it matches the background pressure. At 20 Pa background pressure, $n_{H_2}=3\times10^{21}$ m^{-3} and $T_{rot}=500-600$ K in the surrounding of the plasma jet.

III. H ATOM DENSITY AND TEMPERATURE ALONG THE JET CENTERLINE

A. Loss of H atoms by diffusion

As mentioned in the introduction, the flow pattern of H atoms is expected to be governed by wall-recombination processes. As a consequence, it should significantly deviate from the classical expansion behavior as treated by the rarefied gas dynamics theory. The measured ground-state H atom density profile along the plasma jet centerline is shown in Fig. 3 for two different background pressures. The shape of the density profile is indeed in disagreement with the shape expected from the neutral gas supersonic expansion theory. At $p_{back}=20$ Pa, there is no clear evidence of any density jump throughout the stationary shock wave. At $p_{back}=100$ Pa, a density jump with an amplitude of 1.4 is visible. However, this is in disagreement with the expected magnitude, as will be discussed in the next section. The two density profiles reveal a nonconservation of the H atom forward flux throughout the stationary shock wave in contradiction with the well-established Rankine–Hugoniot relations.[18] Behind the shock wave, the H density decreases as shown in Fig. 3, and since the temperature decreases also (see next section), hydrogen atoms do not flow at constant static pres-

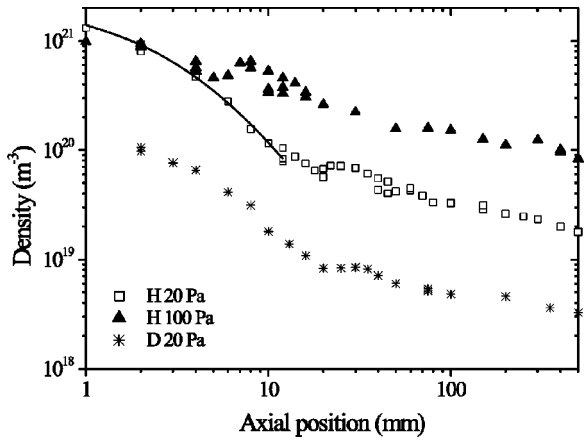

FIG. 3. Ground-state H atom density profile along the jet centerline at $p_{back}=20$ Pa (open square) and $p_{back}=100$ Pa (solid triangle) in standard conditions. Also shown is the ground-state D atom axial density profile at 20 Pa background pressure (star) in the case of a H_2-D_2 mixture (3.1 slm H_2 and 0.4 slm D_2). The solid line represents a fit using Eq. (6).

sure. In Fig. 4, the measured H atom partial static pressure is shown in the subsonic domain for two different background pressures. The static pressure is calculated from the measured density and temperature using the perfect gas law $p=nk_BT$, with k_B the Boltzmann constant. Since the dynamic pressure term can be neglected in the subsonic domain, a decrease in static pressure is connected to a loss of H atoms.

In the supersonic flow regime, the density profile also shows evidence of losses of H atoms. From the flux conservation law in stationary state, and under the assumption that the particles originate from a point source and flow along straight stream lines, one can obtain a theoretical expression for the density behavior inside the supersonic domain along the jet centerline. The particle density as a function of the distance $n(z)$ is given by

$$n(z)=n_o\frac{z_{\mathrm{ref}}^{\beta}}{(z+z_{\mathrm{source}})^{\beta}}. \tag{6}$$

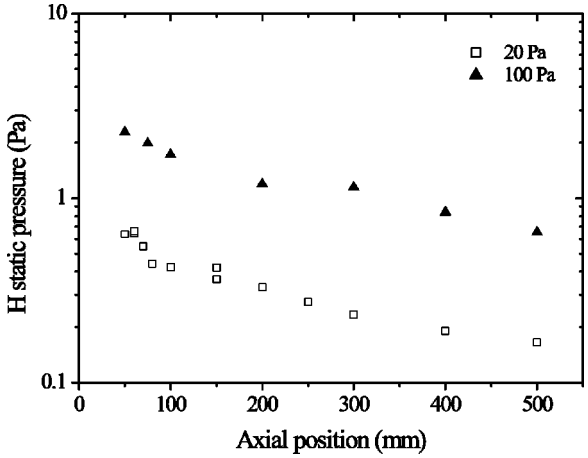

FIG. 4. Measured atomic hydrogen static pressure along the jet axis in the subsonic domain of the plasma expansion at two different background pressures. Contrary to inert neutrals, radicals are not transported at constant static pressure behind the shock region meaning that they diffuse out of the plasma jet.

In Eq. (6), n_o is the density at the origin of the expansion, z_{ref} is a scaling length and z_{source} is the position of the virtual point source. The exponent β defines the steepness of the density decrease. In the case of a supersonic expansion of an inviscid gas through a sonic orifice, it is shown that the exponent β is equal to 2, which corresponds to the classical rarefaction effect.[16,23] The same value of 2 also applies in the case of the transport of neutral atoms in a plasma expansion.[24] From a fit of the H density profile ahead of the shock wave using Eq. (6) we find that $z_{\mathrm{source}}=+(4\pm1)$ mm and $\beta=2.4\pm0.2$ at $p_{\mathrm{back}}=20$ Pa (see Fig. 3). Moreover, we find that $z_{\mathrm{ref}}=(3.5\pm1.5)$ mm, in the order of the nozzle diameter as expected, and $n_o=(3.5\pm1.5)\times10^{21}$ m^{-3}. First, the expansion of H atoms starts already inside the plasma source nozzle, which is unexpected in the case of a straight nozzle. Second, the H density drop is faster than the expected one, meaning that a loss mechanism is superimposed onto the rarefaction effect. In a previous work devoted to the study of the transport of H atoms in an $Ar-H_2$ plasma, β is found to be larger than 2 and pressure dependent, and it approaches 2 at high background pressure.[8]

Even if ground-state hydrogen atoms can recombine in volume due to the following three-body reactions:

$$H+H+H_2\rightarrow H_2+H_2 \quad \text{and} \quad H+H+H\rightarrow H_2+H, \tag{7}$$

the reaction rates (see, for example, Ref. 25), however, are too low to lead to any significant loss of H atoms under our experimental conditions. Therefore, the observed anomalous transport of H atoms arises from the fact that H escapes the plasma jet in the course of the expansion. As shown in previous papers,[7,8] the loss of H atoms is a direct consequence of the existence of large density gradients between the core of the plasma jet and its surroundings. The low H atom concentration in the background gas, which is responsible for an outward diffusion of H radicals, results from the very efficient destruction of H atoms at the reactor walls when a high wall-recombination probability (Γ) is combined with a long residence time (τ). The wall-recombination probability on stainless steel for H atoms is known to be large: $\Gamma_{ss}=0.1-0.2$[26,27] at temperature close to room temperature. The coefficient Γ depends on the surface temperature,[28] on the state of the surface (roughness, presence of impurities, coverage by H) and on the energy of the incident H atom. That indicates how difficult it is to have an accurate estimate of Γ. Moreover, the residence time inside our vacuum vessel is relatively long: $\tau\approx0.8$ s at 20 Pa and $\tau\approx4$ s at 100 Pa. That makes high losses of H radicals at the vessel walls, and thus a low H atom density in the background, very probable.

B. Perpendicular temperature development

The perpendicular temperature ($T_\perp$) profile of the H atoms along the jet centerline is plotted in Fig. 5 for two different background pressures. Due to conversion of thermal energy into kinetic energy, i.e., directed motion, the H temperature drops quickly in the supersonic domain. The temperature profiles clearly reveal the occurrence of a stationary shock wave across which the temperature rises because of collisions with the background gas particles. As can be seen

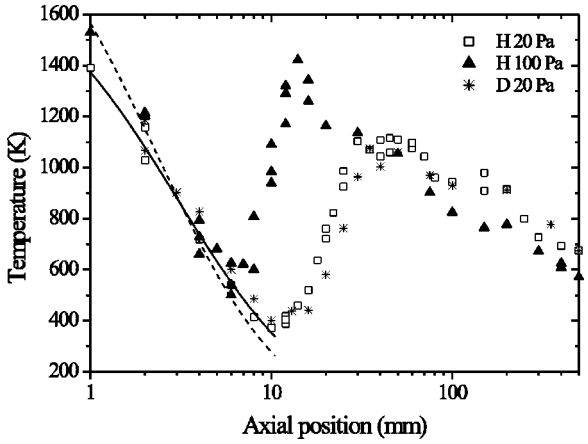

FIG. 5. Ground-state H atom perpendicular temperature ($T_\perp$) profile along the jet centerline at $p_{back}=20$ Pa (open square) and $p_{back}=100$ Pa (solid triangle) in standard conditions. Also shown is the atomic deuterium axial $T_\perp$ profile at 20 Pa background pressure (star) for a H_2-D_2 mixture (3.1 slm H_2 and 0.4 slm D_2). The measured H and D axial temperature profiles at 20 Pa are similar. The theoretical H atom temperature profile within the supersonic domain is shown at 20 Pa using $\gamma=1.55$ (solid line) and $\gamma=5/3$ (dashed line).

in Fig. 5 both the position and the thickness of the shock wave depend on p_{back}. In the subsonic part of the expansion, the temperature decreases due to heat transfer to the vessel walls. Behind the shock region, the measured H atom temperature is in good agreement with the H_2 rotational temperature. The numerous collisions in the subsonic domain enable to maintain thermal equilibrium between H and H_2.

Using the Poisson adiabatic law, the temperature at the origin of the H atom expansion T_o as well as the isentropic exponent γ can be determined from a plot of the H temperature as a function of the H density in the supersonic domain. It is found that $\gamma=1.55\pm0.05$ at $p_{back}=20$ Pa and $\gamma\approx1.7$ at $p_{back}=100$ Pa. At 20 Pa background pressure the plasma expansion is found to be non-adiabatic, since γ is smaller than its adiabatic value 5/3, as shown in Fig. 5. The fact that the supersonic expansion is not an adiabatic process may be explained by heat transfer from both the plasma source and the hot gas located behind the shock region. Another possibility is the entry in the jet of hot H_2 molecules, coming from the surrounding gas, in the last part of the supersonic domain where the mean free path for momentum exchange is large. The fact that the measured γ does not contain any molecular effects whereas the jet is mainly composed of H_2 ($\gamma_{mixture}\approx1.3$) is an indication in favor of a strong decoupling between H atoms and H_2 molecules during the expansion process. The temperature T_o is equal to 2500 ± 500 K. This temperature corresponds to the H temperature inside the arc nozzle, since $z_{source}=+4$ mm with this geometry. Therefore, the temperature inside the nozzle is different from the temperature inside the arc channel, which is about 1.2 eV.[29] In fact the plasma starts to cool down already in the arc nozzle and this drop in temperature may have a non-negligible influence on plasma processes like ion-recombination for instance.

C. Injection of molecular deuterium in the arc

In order to study the influence of the mass on the transport of radicals and particularly on the confinement of radicals inside the jet, deuterium is added to the hydrogen flow and the created D atoms are monitored in the H_2-D_2 expanding plasma. The flow mixture is composed of 3.1 slm H_2 and 0.4 slm D_2. The cascaded arc parameters stay unchanged.

The perpendicular temperature profile of deuterium atoms along the jet axis, measured at $p_{back}=20$ Pa, is shown in Fig. 5, together with the temperature profile of H atoms. Both profiles indicate the same shock wave location and width. In the supersonic domain, as well as in the subsonic domain, H and D temperature profiles overlap reasonably. Throughout the stationary shock wave, the D atom $T_\perp$ is lower than the H atom $T_\perp$ by approximately a factor 1.2. This departure from thermal equilibrium in the shock region is not yet well understood. It may be caused by a difference in energy exchange in a $D-H_2$ collision as compared to an $H-H_2$ collision, H_2 molecules being the main collision partner.

The deuterium atom density profile for an H_2-D_2 plasma at a pressure of 20 Pa is compared to the hydrogen atom density profile for a pure H_2 plasma in Fig. 3. At the plasma source outlet, the ratio of the H density to the D density is approximately equal to the injected gas flow ratio. This supports the idea of a high-dissociation degree and an efficient mixing inside the arc channel where the plasma is created. In the supersonic domain, we obtain $\beta=2.0\pm0.1$ and $z_{source}=+(4\pm1)$ mm when using Eq. (6) to describe the density drop. The value of the exponent β is close to the value characteristic for a neutral gas supersonic expansion. Deuterium atoms are well coupled to H_2 molecules, as expected in view of the equal mass of the two particles, and thus they are relatively well confined inside the plasma jet, as indicated by the value of β. When the jet is underexpanded, losses of D atoms can, however, occur in the barrel shock, i.e., at the sides of the jet, where the mean free path is large and the radial velocity high. Across the stationary shock wave, the forward D atom flux is not conserved. In the shock region D atoms can escape the plasma jet because of the large mean free path. In the subsonic region, the confinement of D is better than that of H, nevertheless D atoms are lost. The mass of the particle plays a role in the transport mechanism, since the loss of radicals arises from a diffusion process. It is shown, however, that when the mass of the carrier gas is close to that of the radicals the confinement inside the jet is improved but the losses by diffusion cannot be avoided if the wall-recombination probability is high.

IV. RECOMBINATION IN THE ARC NOZZLE

From the measured H atom density and axial velocity it is possible to estimate the plasma source dissociation degree δ. This parameter characterizes the source strength, i.e., the capability of producing H radicals. The dissociation degree can be expressed as follows:

$$\delta = \frac{\phi_{\mathrm{H}}}{2\,\phi^{\mathrm{o}}_{\mathrm{H}_2}}, \tag{8}$$

where ϕ_{H} is the ground-state atomic hydrogen flux and $\phi^{\mathrm{o}}_{\mathrm{H}_2}$ the gas flow of molecular hydrogen at the arc inlet. Under our experimental conditions, $\phi^{\mathrm{o}}_{\mathrm{H}_2} = 1.56\times 10^{21}\ \mathrm{s}^{-1}$. At the origin z_o of the H atom expansion, i.e., inside the arc nozzle, $\delta \approx 0.1$, if the plasma is assumed to flow with the local speed of sound. Just behind the source exit ($z = 1$ mm), $\delta \approx 0.04$ when the velocity profile over the jet radius is assumed to be flat. In our conditions, the low value of δ does not arise from volume recombination of H atoms in view of the low three-body reaction rates.[25] For comparison, the dissociation degree in the background is found to be less than 1%. In that case the H_2 density is deduced from the static pressure using the H atom temperature ($T_{\mathrm{H}} = T_{\mathrm{H}_2}$ in the background, see Sec. VI). The low value of δ in the downstream part of the flow is a direct consequence of the loss of H by diffusion during the expansion process. However, such a low-dissociation degree in the source is not expected at an electron temperature of around 1 eV.

To a large extent, the low source dissociation degree can be connected with the low-electron density observed in the case of an expansion of a hydrogen plasma.[14,15] As already mentioned, the emerging plasma is dark. It thus appears that the expanding plasma jet is mainly composed of H_2 molecules. The low value of δ as well as the ionization loss need further clarification. A possible way to explain this experimental fact is to consider the production of vibrationally excited hydrogen molecules (in the electronic ground-state) on a surface. Neutral hydrogen atoms can indeed recombine on a surface to form excited H_2 molecules

$$\mathrm{H_{gas}} + \mathrm{H_{ad}} \rightarrow \mathrm{H}_{2\mathrm{gas}}^{v,J}. \tag{9}$$

This chemical reaction has been extensively studied both experimentally and theoretically (see for instance Refs. 30–32). Because the probability for recombinative desorption of H atoms on a Cu surface is close to unity,[28,32] H atoms can easily be lost via the previous reaction in the arc nozzle, which is made of Cu. Accordingly, a large amount of $H_2^{v,J}$ molecules can be generated. Atomic hydrogen ions H^+, the most abundant ion, can easily exchange their charge with vibrationally excited H_2 molecule leading to H_2^+ ions (see Sec. II A). The dissociative recombination of H_2^+ molecular ions is the main source of visible light (H_α radiation).

Inside the arc nozzle, recombination processes are favored. In the standard cascaded arc configuration, the nozzle acts as the anode. The arc root, however, attaches at the nozzle inlet (nozzle length = 17 mm) and thus no energy is supplied in the largest part of the nozzle. Therefore, surface-recombination of H atoms and the subsequent $H_2^{v,J}$ formation can explain the low value of both the dissociation degree and the ionization degree at the arc exit: H atoms are lost at the nozzle wall and the created H_2^+ ions recombine before they escape the source. The fact that no significant amounts of rovibrationally excited H_2 molecules are measured in the plasma jet supports the idea that most of $H_2^{v,J}$ molecules produced in the arc nozzle by wall-recombination of H atoms may be quickly lost via the formation of H_2^+ ions (that explains the absence of visible light). As it appears, the process of surface-recombination in the arc nozzle is complex, but it certainly needs further investigation, since it plays a decisive role if the plasma jet is to be used as an efficient H ion or H radical source.

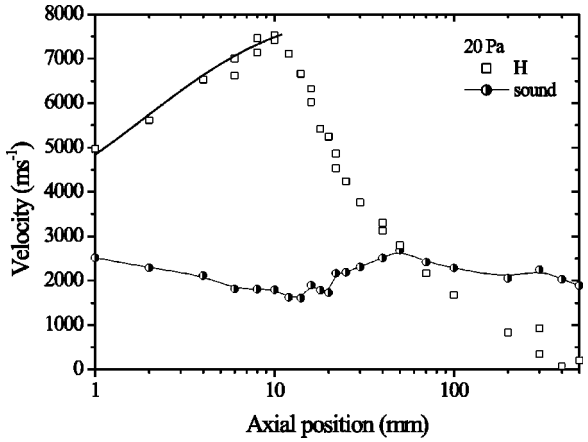

FIG. 6. Development of the atomic hydrogen axial velocity component (w_z) along the jet axis at $p_{\mathrm{back}} = 20$ Pa (open square) and speed of sound (c_s) calculated from the measured parallel temperature ($T_{\parallel}$) with $m = 2$ amu (circle). The Mach number in front of the shock wave is equal to 4. The solid line is the outcome of a simple theoretical model describing the H axial velocity in the supersonic domain, see Eq. (12).

V. AXIAL VELOCITY COMPONENT AND SOUND SPEED

Another important parameter to be determined in order to characterize the atomic radical transport mechanism is the flow velocity. The measured H atom axial velocity component profile along the jet centerline is shown in Figs. 6 and 7 at 20 and 100 Pa background pressure, respectively. Throughout the stationary shock wave, the velocity distribution function is found to be non-Maxwellian. The study of the departure from thermodynamic equilibrium in the shock region of an expanding plasma will be reported in a coming

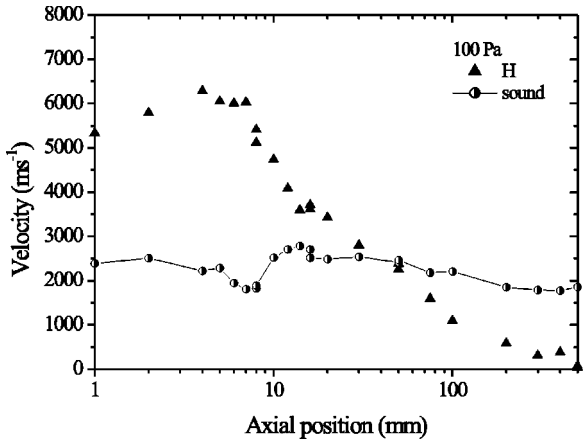

FIG. 7. Development of the atomic hydrogen axial velocity component (w_z) along the jet axis at $p_{\mathrm{back}} = 100$ Pa (solid triangle) and speed of sound (c_s) calculated from the measured parallel temperature ($T_{\parallel}$) with $m = 2$ amu (circle). The Mach number in front of the shock wave is equal to 3.

paper. In this contribution we only consider the averaged axial velocity in the shock region, i.e., the velocity calculated from the first moment of the distribution function. To clearly discern the three different flow regimes (supersonic, shock, subsonic), the flow velocity has to be compared with the local speed of sound in order to obtain the Mach number. The speed of sound is given by

$$c_s = \sqrt{\frac{\gamma k_B T}{m}}, \tag{10}$$

where γ is the adiabatic exponent and k_B the Boltzmann constant, and m the mass. The Mach number M reads

$$\mathrm{M} = \frac{w}{c_s}, \tag{11}$$

where w is the flow velocity. The on-axis development of the speed of sound is plotted in Figs. 6 and 7 for two different background pressures using the measured H atom parallel temperature ($T_\parallel$), the temperature associated with the velocity distribution parallel to a stream line, and using as mass number $m=2$ amu since H_2 is the major component of the jet. The sound speed at the expansion origin z_o inside the arc nozzle can be calculated using T_o: $c_{s,o} \approx 4100$ ms^{-1}. At the plasma source exit the Mach number is already high, M = 2. A theoretical expression describing the evolution of the axial velocity along a stream line in the supersonic domain can be obtained from the Bernoulli equation and the Poisson adiabatic law.[33] If we consider that the plasma starts to expand with $c_{s,o}$, one finds for the velocity

$$w(z) = \frac{c_{s,o}}{\sqrt{\gamma-1}} \sqrt{\gamma+1-2\left(\frac{n(z)}{n_o}\right)^{\gamma-1}}$$

$$= \frac{c_{s,o}}{\sqrt{\gamma-1}} \sqrt{\gamma+1-2\left(\frac{z_{\mathrm{ref}}}{z+z_{\mathrm{source}}}\right)^{\beta(\gamma-1)}}, \tag{12}$$

when Eq. (6) is used to express the density as a function of z. Since the previous expression contains β it accounts automatically for the outward diffusion effect when $\beta > 2$. In Fig. 6 the measured H atom axial velocity profile in the supersonic domain at 20 Pa is compared with a calculation using Eq. (12). The agreement is satisfactory. The Mach number at the source exit is equal to 2 for the two background pressures. As can be seen from Eq. (12) the maximum flow velocity only depends on T_o and accordingly on the source temperature. In our conditions, $w_{\max} = 8200$ ms^{-1}. However, before the hydrogen atoms can reach the maximum velocity they start colliding with the residual background gas, meaning that the expansion never enters the so-called frozen regime.[17] Because of the poor confinement of H atoms inside the jet, H atoms and H_2 molecules are not perfectly coupled. As a consequence, the H velocity can be slightly higher than the H_2 velocity in the supersonic domain because of the addition of a diffusion term.[8]

The existence of a stationary shock wave is clearly revealed in Figs. 6 and 7. In the two figures, the effect of the background pressure on both the shock wave position and the shock wave thickness is visible. The Mach disk location z_{M} is found to be equal to 50 mm at 20 Pa and 30 mm at 100 Pa. A calculation using Eq. (5) gives: $z_{\mathrm{M}} = 74$ mm and $z_{\mathrm{M}} = 33$ mm at 20 and 100 Pa, respectively. The poor agreement at low background pressure arises from the fact that the dynamic pressure at the Mach disk is not taken into account in the calculation and this pressure term is not negligible in comparison with static pressure when the background pressure is low. At $p_{\mathrm{back}} = 20$ Pa, the measured shock thickness is equal to 40 mm. It can be compared with the H–H_2 collision mean free path ahead of the shock region, since H atoms mainly collide with H_2 molecules. The mean free path is given by

$$\lambda_{\mathrm{H-H_2}}^{mfp} = \frac{1}{n_{\mathrm{H_2}} \sigma_{\mathrm{H-H_2}}}, \tag{13}$$

where $n_{\mathrm{H_2}}$ is the molecular hydrogen density and $\sigma_{\mathrm{H-H_2}}$ the momentum exchange cross section. The H_2 density has been measured: $n_{\mathrm{H_2}} \approx 5 \times 10^{20}$ m^{-3} at 20 Pa. The value for the cross section can be found in literature;[34] at 500 K $\sigma_{\mathrm{H-H_2}} = 2 \times 10^{-19}$ m^2. At 20 Pa a mean free path for momentum exchange ahead of the shock wave of 12 mm is found. Thus the shock wave thickness is in the order of few $\lambda_{\mathrm{H-H_2}}^{mfp}$. At this pressure the mean free path becomes in the order of the jet dimension (10 mm radius at $z = 10$ mm if a 45° expansion is assumed). Therefore, at this point the flow cannot be satisfactorily described using the hydrodynamic theory and one must turn to the more complex gas kinetic theory.

The Mach number ahead of the stationary shock wave can be deduced from our measurements: M=4 at 20 Pa and M=3 at 100 Pa. Using the Rankine–Hugoniot relations both the theoretical density and temperature jump across the shock wave can be calculated using these Mach numbers. With an adiabatic exponent of 1.55, the expected density jump is equal to 3.6 at 20 Pa and 3.2 at 100 Pa in complete disagreement with the measured value (see Fig. 3). The observed discrepancy is a direct consequence of the losses of H atoms by diffusion. The calculated temperature jump is equal to 5.9 at 20 Pa and 3.4 at 100 Pa, whereas the measured jump is equal to 3.3 and 2.7 at 20 Pa and 100 Pa, respectively. Too small a temperature jump across the shock wave confirms the idea of the invasion of the shock region by the surrounding background gas. The resulting energy transfer modifies the temperature.

Behind the stationary shock wave, the velocity decreases because of momentum transfer to the background gas particles.

VI. PLASMA JET VICINITY

In order to evaluate the difference in the H atom concentration and temperature between the core of the jet and the surrounding background gas, it is of interest to study jet cross sections. The radial profile of the H atom density as well as the corresponding temperature profile have been measured at an axial position z of 30 mm from the arc outlet, i.e., in the shock region, at $p_{\mathrm{back}} = 20$ Pa.

The density profile is shown in Fig. 8. In the core of the jet the H density is high, $n_{\mathrm{H}} = 6 \times 10^{19}$ m^{-3} whereas it is relatively low in the jet vicinity, $n_{\mathrm{H}} \approx 10^{19}$ m^{-3}. Therefore, in

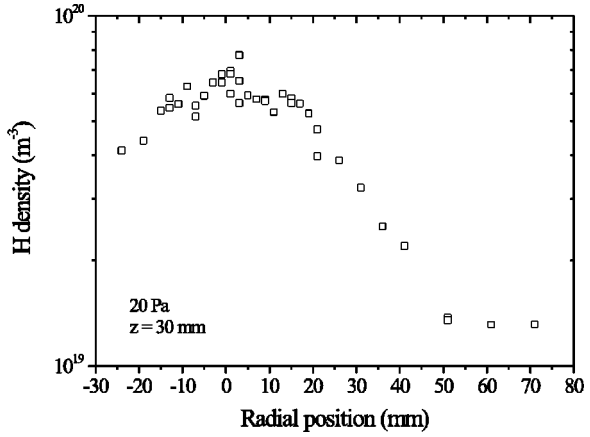

FIG. 8. Radial profile of the H atom density at 20 Pa background pressure measured at 30 mm behind the arc outlet. The H density outside the jet is relatively low due to wall-recombination processes. For comparison, the H_2 density around the plasma jet (background) is around 3×10^{21} m^{-3} at 20 Pa.

the shock wave zone the H radical expansion is not overexpanded, contrary to that of nonreacting neutrals. As mentioned previously, the low H density in the background is a consequence of the recombination of H atoms at the walls of the vacuum chamber. For comparison, the background molecular hydrogen density at 20 Pa is about 3×10^{21} m^{-3}. The existence of strong density gradients at the jet boundary supports the idea of an outward diffusion process.

The radial profile of the H atom perpendicular temperature is shown in Fig. 9. The temperature is on the average relatively high in the core of the jet, approximately 1100 K, however it is slightly lower around the jet axis. Indeed at $r\approx0$, a dip is visible in the temperature profile in Fig. 9. The temperature is higher at the jet boundary because of collisions with the background gas. The temperature gradually decreases in the vicinity of the plasma jet to about 500 K due to heat transfer to the vessel wall. The measured H atom background gas temperature is in good agreement with the H_2 rotational temperature.

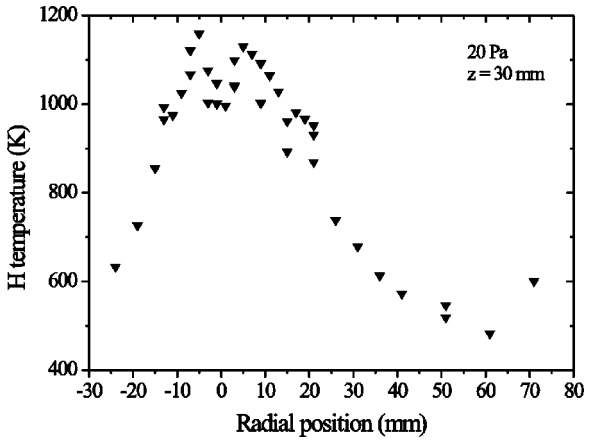

FIG. 9. Radial profile of the H atom perpendicular temperature at 20 Pa background pressure and at 30 mm behind the arc outlet. The H_2 rotational temperature in the background is found to be 500–600 K (Ref. 22), in good agreement with the H temperature at large r.

VII. CONCLUSION

The study of the transport of ground-state hydrogen atoms in the expansion of a thermal hydrogen plasma reveals that surfaces can have a great influence on the chemistry and on the dynamics of a system containing reactive particles. The low dissociation degree, as well as the quasi-absence of charged particles at the plasma source exit, can be explained by the recombination of H atoms on the arc nozzle wall and the subsequent formation of vibrationally excited hydrogen molecules. More striking, the transport of H atoms is also strongly influenced by surface-recombination processes. The efficient loss of H atoms at the vessel walls creates large density gradients between the jet and the surroundings, which in turn force H to diffuse out of the plasma jet. It is shown that when the surface loss probability is high, i.e., combination of a large wall-recombination probability with a long residence time, the losses of radicals by diffusion cannot be avoided, even when the mass of the carrier gas is close to the mass of the radical.

This work stresses the importance of plasma–wall interactions in the manufacture of a plasma source with specific requirements, but also in the design of reactors devoted to plasma-assisted chemistry. Nowadays the transport of radicals in a plasma expansion is beginning to be better understood, and technological solutions can be proposed in order to enhance the confinement inside the plasma jet (e.g., by using a vessel wall material with a low surface-recombination probability). Nevertheless, further investigations have to be performed on plasma–wall interactions and the related generation of molecules. To better understand the dynamics of the process and to investigate the possibility of using a surface as a catalyst to favor the production of a desired molecule are examples. This may open in the near future a new field in plasma-aided chemistry.

ACKNOWLEDGMENTS

The authors would like to acknowledge fruitful discussion with Professor M. C. M. van de Sanden. The authors greatly appreciate the skillful technical assistance of M. J. F. van de Sande, A. B. M. Hüsken, and H. M. M. de Jong.

This work is part of the research program of the Netherlands Foundation for Fundamental Research on Matter (FOM). It is financially supported by the Netherlands Organization for Scientific Research (NWO) as well as the Euratom foundation.

[1] *Beams and Jets in Astrophysics*, edited by P. A. Hugues (Cambridge University Press, Cambridge, 1991).
[2] J. Wesson, *Tokamak* (Clarendon, Oxford, 1997).
[3] W. M. M. Kessels, M. C. M. van de Sanden, and D. C. Schram, J. Vac. Sci. Technol. A **18**, 2153 (2000).
[4] A. J. T. Holmes, Plasma Phys. Controlled Fusion **34**, 653 (1992).
[5] J. Winter, Plasma Phys. Controlled Fusion **38**, 1503 (1996).
[6] U. Samm and the TEXTOR-94 Team, Plasma Phys. Controlled Fusion **41**, B57 (1999).
[7] S. Mazouffre, M. G. H. Boogaarts, J. A. M. van der Mullen, and D. C. Schram, Phys. Rev. Lett. **84**, 2622 (2000).
[8] S. Mazouffre, M. G. H. Boogaarts, I. S. J. Bakker, P. J. W. Vankan, R. Engeln, and D. C. Schram, Phys. Rev. E **64**, 016411 (2001).
[9] G. M. W. Kroesen, D. C. Schram, and J. C. M. de Haas, Plasma Chem. Plasma Process. **10**, 551 (1990).

[10]M. Capitelli, M. Dilonardo, and E. Molinari, Chem. Phys. **20**, 417 (1977).
[11]M. A. Cacciatore, M. Capitelli, and R. Celiberto, Nucl. Fusion Suppl. **2**, 65 (1992).
[12]H. Tawara, Y. Itikawa, N. Nishimura, and M. Yoshino, J. Phys. Chem. Ref. Data **19**, 617 (1990).
[13]A. Ichihara, O. Iwamoto, and R. K. Janev, J. Phys. B **33**, 4747 (2000).
[14]M. J. de Graaf, R. Severens, R. P. Dahiya, M. C. M. van de Sanden, and D. C. Schram, Phys. Rev. E **48**, 2098 (1993).
[15]R. F. G. Meulenbroeks, R. A. H. Engeln, M. N. A. Beurskens, R. M. J. Paffen, M. C. M. van de Sanden, J. A. M. van der Mullen, and D. C. Schram, Plasma Sources Sci. Technol. **4**, 74 (1995).
[16]H. Ashkenas and F. S. Sherman, *Proceedings of Rarefied Gas Dynamics* (Academic, New York, 1966), Vol. 4, p. 84.
[17]D. R. Miller, *Atomic and Molecular Beam Methods*, edited by G. Scoles (Oxford University Press, New York, 1988), p. 14.
[18]P. A. Thomson, *Compressible-fluid Dynamics* (McGraw-Hill, New York, 1972).
[19]U. Czarnetzki, K. Miyazaki, T. Kajiwara, K. Muraoka, M. Maeda, and H. F. Döbele, J. Opt. Soc. Am. B **11**, 2155 (1994).
[20]H. W. P. van der Heijden, M. G. H. Boogaarts, S. Mazouffre, J. A. M. van der Mullen, and D. C. Schram, Phys. Rev. E **61**, 4402 (2000).
[21]K. Niemi, V. Schultz von der Gathen, and H. F. Döbele, *Proceedings of Hakone* **7** (Greifswald, Germany, 2000), Vol. 1, p. 199.
[22]R. F. G. Meulenbroeks, R. A. H. Engeln, J. A. M. van der Mullen, and D. C. Schram, Phys. Rev. E **53**, 5207 (1996).
[23]H. C. W. Beijerinck, R. J. F. van Gerwen, E. R. T. Kerstel, J. F. M. Martens, E. J. W. van Vliembergen, M. R. Th. Smits, and G. H. Kaashoek, Chem. Phys. **96**, 153 (1985).
[24]M. C. M. van de Sanden, J. M. de Regt, and D. C. Schram, Plasma Sources Sci. Technol. **3**, 501 (1994).
[25]N. Cohen and K. R. Westberg, J. Phys. Chem. Ref. Data **2**, 531 (1983).
[26]M. Mazetič, M. Drobnič, and A. Zalar, Appl. Surf. Sci. **144**, 399 (1999).
[27]P. Kae-Nume, J. Perrin, J. Jolly, and J. Guillon, Surf. Sci. Lett. **360**, L495 (1996).
[28]B. Freiesleben Hansen and G. D. Billing, Surf. Sci. Lett. **73**, L333 (1997).
[29]G. Janssen, ''Design of a General Plasma Simulation Model,'' Ph.D. thesis, Eindhoven University of Technology, The Netherlands (2000).
[30]R. I. Hall, I. Čadež, M. Landau, F. Pichou, and C. Shermann, Phys. Rev. Lett. **60**, 337 (1988).
[31]P. J. Eenshuistra, J. H. M. Bonnie, J. Los, and H. J. Hopman, Phys. Rev. Lett. **60**, 341 (1988).
[32]B. Jackson and M. Persson, J. Chem. Phys. **96**, 2378 (1992).
[33]D. C. Schram, S. Mazouffre, R. Engeln, and M. C. M. van de Sanden, *Atomic and Molecular Beams*, edited by R. Campargue (Springer, New York, 2001), p. 209.
[34]A. Phelps, J. Phys. Chem. Ref. Data **19**, 653 (1996).